A NEW TREATMENT OF THE ALBEDO RADIATION PRESSURE IN THE CASE OF A UNIFORM ALBEDO AND OF A SPHERICAL SATELLITE

NICOLE BORDERIES
Observatoire Midi-Pyrénées, 14 Avenue Edouard Belin
31400 Toulouse, France
and
Jet Propulsion Laboratory 301-150, 4800 Oak Grove Drive
Pasadena, CA 91109, U.S.A.
E-mail NJB@GROUCH.SPAN

PIERRE-YVES LONGARETTI
Observatoire Midi-Pyrénées, 14 Avenue Edouard Belin
31400 Toulouse, France
E-mail LONGARET@FROMP51.BITNET

(Received : 17 April 1990; accepted : 13 September 1990)

Abstract. The purpose of this paper is to present a model for the radiation pressure acceleration of a spherical satellite, due to the radiation reflected by a planet with a uniform albedo. A particular choice of variables allows one to reduce the surface integrals over the lit portion of the planet visible to the satellite to one-dimensional integrals. Exact analytical expressions are found for the integrals corresponding to the case where the spacecraft does not "see" the terminator. The other integrals can be computed either numerically, or analytically in an approximate form. The results are compared with those of Lochry (1966). The model is applied to Magellan, a spacecraft orbiting Venus.

Keywords : Perturbations, radiation pressure, albedo

1. Introduction

Orbits of artificial satellites of the Earth or of other planets must be determined with more and more accuracy, particularly for geodynamics studies. At a level of accuracy of a few centimeters, planetary radiation pressure cannot be ignored.

The first goal of this article is to describe a model for the pressure exerted on a spherical satellite orbiting a planet, due to the solar radiation reflected by the planet, and using the approximation of a uniform albedo. The second goal is to present an application of this model to Magellan, a spacecraft orbiting Venus.

A more general model is presented in a subsequent article, for the case where the satellite surface consists of a number of plane elements, and where the albedo of the planet is expanded in spherical harmonics. The effect of the thermal radiation from the planet is also included in the general model, and treated in a parallel way. The reason to publish the simpler model is that it yields a more elegant derivation and representation of the radiation pressure acceleration than those obtained by

Celestial Mechanics and Dynamical Astronomy **49**: 69–98, 1990.

considering a special case of the general model, and also than those previously published for the same problem.

The plan of the paper is as follows. Section 2 describes the background of the planetary radiation pressure problem, and discusses some particularly significant models. This section is intended to serve as a presentation of the problem for both this article and the subsequent article on the general model. In section 3, we derive the basic equation for the radiation pressure. The model is presented in section 4, and its application to Magellan is presented in section 5. Section 6 summarizes the main results.

2. Background

First, we recall the basic physical processes involved in the radiation pressure acceleration. Then, we characterize the acceleration as small and difficult to represent analytically. While comparable forces, such as those deriving from minute tesseral harmonics coefficients of the Earth's gravity field, were correctly taken into account thirty years ago, planetary radiation pressure has been most often either ignored in force models or introduced with drastic approximations. We examine the motivations for constructing models of planetary radiation pressure and the approaches which have been used.

2. 1. BASIC PHYSICAL PROCESSES

Electromagnetic radiation can be decomposed into a spectrum of waves. Each wave is characterized by its frequency ν, related to its wavelength λ by $\lambda\nu = c$, where $c \simeq 3.00\ 10^8$ m s^{-1} is the free space velocity of light. The energy of one photon is $E = h\nu$, where $h = 6.626\ 10^{-34}$ J s is Planck's constant. The temperature associated with each wavelength is defined by $T = E/k$, where $k = 1.380\ 10^{-23}$ J K^{-1} is Boltzmann's constant. The momentum of the photon is $\vec{q} = E/c\ \hat{q}$, where $\hat{q}$ is the unit vector in the direction of the photons' motion. Radiation can exert a force through the exchange of momentum between photons and matter.

Let us consider a surface element dS exposed to radiation. The interaction of the surface element with this radiation can be decomposed into four processes :

1. the surface element is struck by the incoming photons which transmit their momentum to dS.
2. a fraction of the incident photons is reflected specularly, and dS loses the corresponding momentum;
3. a fraction of the incident photons is reflected diffusively, and dS loses the corresponding momentum;
4. the remaining incident photons are absorbed and heat the matter; the surface emits energy at a rate of $\epsilon\sigma_0 T^4$, per second per cm^2 where ϵ is the emissivity of dS and $\sigma_0 = 5.671\ 10^{-8}$ W m^{-2} K^{-4} is the Stefan-Boltzmann constant.

The same processes govern the way in which a planet radiates energy. Part of this energy consists of solar radiation immediately reflected by the planet, in the

same waveband as the solar radiation, that is to say with wavelengths between 0.2 and 4.0 μm. This waveband includes ultraviolet radiation (below 0.38 μm), all the visible light (between 0.38 and 0.75 μm) and near infrared radiation (above 0.75 μm). The ratio of the flux reflected in all directions to the incident flux is the albedo. The other part of the planetary radiation consists of thermal emission associated with the temperature of the planet. The wavelength of the peak of thermal emission can be characterized in the following way. The monochromatic specific intensity $B_\lambda(T)$ radiated by a body that is at uniform temperature T and in thermodynamic equilibrium varies with the wavelength λ according to Planck's law : $B_\lambda(T) = (2hc^2/\lambda^5)/[(\exp(hc/\lambda kT) - 1]$. The wavelength λ_{max} at which the maximum of $B_\lambda(T)$ occurs is given by Wien's displacement law : $\lambda_{max}T = 0.29$ cm K. For a body with a temperature of 290 K, the average temperature of the Earth, $\lambda_{max} = 10$ μm. The thermal radiation emitted by the planets occurs in the infrared waveband.

The same processes also occur for an artificial satellite of a planet. Each element of surface dS of the orbiter may be exposed to radiation coming from the Sun, from the planet, and from other parts of the spacecraft. The incoming radiation, the radiation reflected specularly and diffusively, and the thermal emission by dS, all exert force on the spacecraft.

2. 2. CHARACTER OF PLANETARY RADIATION PRESSURE

2. 2. 1. A SMALL MAGNITUDE

Perturbations due to planetary radiation are small, typically on the order of 10% of those associated with direct solar radiation pressure. Moreover, the constant term of the thermal flux produces an undetectable effect, equivalent to a small reduction of the gravitational force.

2. 2. 2. COMPLEXITY

Planetary radiation pressure is also difficult to represent. There are two major difficulties.

(i) The first difficulty arises from the fact that the source of radiation is extended, which leads to expression of the acceleration components in the form of surface integrals "defying a simple analytical solution" (Smith, 1970). Only the lit portion of the planet visible to the satellite contributes to the acceleration, and this complicates the limits of integration.

(ii) The second difficulty lies in evaluating the amount of radiation coming from a given location on the planet. We specialize the discussion to the Earth, on which most of the research has concentrated.

We do not know precisely how much radiation coming from the Earth is due to specular reflection of solar light, and how much is due to diffuse reflection. Observing that specular reflection can really be expected only from very calm seas or lakes, while clouds, snow fields and the continents all tend to produce

diffuse reflection, Smith (1970), estimates that the specular albedo of the Earth is about 0.04, that is to say only about 10 % of the total Earth albedo. Furthermore, Knocke and Ries (1987) reason that since the Earth reflection is essentially diffuse at small solar zenith angles and more anisotropic at larger solar zenith angles (Taylor and Stowe, 1984), and since Earth elements at large solar zenith angles do not contribute much to the radiation pressure, Earth radiation pressure may be calculated to acceptable accuracy using a diffuse reflection model.

Another aspect of the problem is that the albedo of a planet varies with latitude, longitude and time. The albedo of the Earth is due to a large degree to the cloud cover, which is a highly variable phenomenon. Similarly, the thermal emission of a planet depends on the position and the time.

Considering the small magnitude of the planetary radiation pressure and its complex nature, what are the reasons to study it?

2. 3. MOTIVATIONS

The orbits of balloon satellites, because of the large area to mass ratio of these objects, are particularly affected by radiation pressure forces. In the 1960s, analyses of the solar radiation pressure and order-of-magnitude calculations of Earth radiation pressure perturbations on artificial satellites were motivated by these balloon satellites (see Baker, 1966, for a review of the corresponding literature).

The satellite Lageos gave rise to a renewal of interest for the problem of the Earth's radiation pressure. The purpose of this satellite was the measurement of plate motion, polar motion and Earth's rotation from the analysis of the satellite's orbit. A high accuracy orbit was needed to make these measurements possible. Unexpected perturbations in Lageos's orbit, in particular a secular decrease of its semi-major axis of 1.1 mm per day, modulated by long-periodic oscillations, were discovered (Smith and Dunn, 1980). Researchers have investigated and debated the possible causes of these unexpected variations, including radiation pressure due to Earth (Rubincam, 1982, Smith, 1983, Anselmo *et al*, 1983, Morgan, 1984, Barlier *et al*, 1985, Rubincam and Weiss, 1986, Rubincam, 1987, Rubincam *et al*, 1987).

Satellites of the new generation, such as Topex-Poseidon, require more sophisticated models to match the new data. Work on the radiation pressure is needed in order to allow us to meet the accuracy requirements for these satellites.

2. 4. APPROACHES

The very first article dealing with the Earth-reflected radiation received by a satellite is by Levin (1962). Levin writes the flux vector in a reference frame centered on the Earth and such that the y axis is along the direction of the Sun. He studies the "symmetric model" which corresponds to the case where the satellite's orbital plane contains the Sun. One limitation of Levin's calculation is that he considers only the radiation reflected specularly and not the radiation reflected diffusively. A more serious limitation is that he neglects the fact that any reflecting surface $d\sigma$ of the Earth does not generally receive the solar light along its normal. His article

considers the radial and transverse components of the flux vector, leading to the conclusion that components other than in the radial direction generally may be neglected. This conclusion was justified by the accuracy of the orbit determinations in the 1960s.

The first detailed and complete analytical treatment of the problem was made by Baker (1966) for the effect of a uniform albedo and delayed infrared emission by the Earth (thermal emission). Baker's treatment has been refined by Lochry (1966) who considers the case where the albedo has a simple latitudinal variation.

Four comments can be made on the approach of Baker and Lochry :

1. Baker notices that, until his work, researchers "usually overlooked or discounted [...] the fact that the radiation pressure acceleration is *not* necessarily in the same direction as the radiation flux vector". In his equation (13), he takes into account the three aspects of the acceleration exerted on a flat plate corresponding to the incident radiation, the specular reflection, and the diffuse reflection. However, Baker makes an error. Instead of integrating the elementary acceleration exerted by the radiation from a surface element of the Earth, he integrates the flux vector over the effective surface of the Earth. Hence, he computes correctly the flux vector, but not the acceleration vector. His results are still useful for a spherical satellite, because it turns out that the elementary acceleration exerted on a spherical satellite is proportional to the elementary flux vector, but not useful for a flat plate or a more complexely shaped satellite.
2. Baker and Lochry work in a system of coordinate axes $OXYZ$ such that O is the center of the Earth, OX is directed towards the Sun, and the spacecraft is in the OXY plane. This choice of reference frame is interesting because the flux vector lies in the OXY plane. Also, the Sun direction is obviously special in the problem, so that it seems a good idea to use it as direction for one of the axes, although actually the spacecraft direction would have been a better choice for the OX axis. They describe the location of a surface element of the Earth by the longitude α and the latitude δ relative to the $OXYZ$ reference frame. This is not a fortunate choice. As a matter of fact α and δ do not separate in the expression for the elementary flux. In particular, the factor $1/\rho^3$, where ρ is the distance between a surface element on the Earth and the spacecraft, depends on both variables.
3. Because they cannot deal rigorously with the terms in $1/\rho^3$, Baker and Lochry use the expansion of $1/\rho$ in Legendre polynomials as a series of a/r where a is the radius of the Earth, and r is the orbital radius of the spacecraft. In practice, a/r can be close to unity. For instance, when Magellan is at periapse, we have $a/r \simeq 0.96$. The fact that Baker and Lochry limit themselves, from the beginning, to developments in series of this parameter appears as a weakness of their method.
4. Baker studies the perturbations on an artificial satellite by using a numerical integration.

Lautman (1977a) studies the uniform albedo problem for a spherical satellite, and the case where the albedo has a simple latitudinal variation but the termina-

tor is neglected (1977b). In both cases, Lautman starts from Lochry's expressions. What Lautman adds to the work of Lochry is an analytical derivation of the expressions for the perturbations of the orbital elements.

Sehnal (1981) studies the problem of the Earth thermal radiation pressure in the case where the flux of infrared radiation is described with zonal harmonic coefficients of zero and second degree. Sehnal finds a clever choice of variables α and β to describe the location of a surface element on the Earth. With this choice of variables, the quantity $1/\rho^3$ depends only on β, and the integration with respect to α is readily made. The problem is then reduced to the evaluation of one–dimensional integrals. Sehnal chooses not to analytically comput these integrals because his goal is to derive the perturbations of the elements and the expressions resulting from the rigorous integration would be too troublesome for that. So, like the previous authors, he uses a development in series of the ratio of the Earth radius over the orbital radius.

Rubincam and Weiss (1986) produced the most advanced analytic treatment to this day, solving the albedo problem for a spherical satellite in the case where the albedo is developed in spherical harmonics. The major features of their model can be summarized as follows.

1. They write the acceleration as $F = \int_0^{2\pi} d\lambda \int_0^{\pi} d\theta \; G(\theta, \lambda)$, where θ and λ are the colatitude and longitude in an Earth equatorial reference frame. To take into account the fact that the only portion of the Earth which contributes to the acceleration is the intersection of the lit hemisphere with the cap visible to the satellite, they make the integrand a product of two discontinuous functions, equal to zero for all the points which do not belong to the sunlit portion of the Earth visible to the satellite.
2. They write each discontinuous function as an infinite sum of Legendre polynomials, then use the addition theorem of spherical harmonics for each of these functions.
3. The albedo is also developed in spherical harmonics. The integrand is written as a series of products of spherical functions depending on θ and λ, as well as the colatitudes and longitudes of the Sun and the spacecraft. Using spherical harmonic properties, Rubincam and Weiss are able to analytically integrate the expressions for the components of the acceleration.
4. Finally, they express the components in terms of the orbit parameters.

Two comments can be made about this model. The first one is that the resulting expressions are very complicated for practical use. The second comment is that these expressions consist of truncated series, the most severe approximation being the necessarily truncated developments of the two discontinuous functions in Legendre polynomials.

In contrast with the mathematical developments made by Rubincam and Weiss (1986), Milani, Nobili and Farinella (1987) give a discussion of the effects on a satellite's orbit of the Earth-reflected radiation pressure, with an application to the long-periodic perturbations of Lageos' orbit. They stress the importance of the

variations in the reflective properties of the Earth with the latitude and the seasons due to varying sea-land distribution and meteorological conditions, respectively.

Kabeláč (1988) gives a treatment of the Earth scattered and thermal radiation on an artificial satellite. He works in a reference frame which is essentially the same as that of this article. The main limitation of his method is that he neglects the dependence on the angle between the direction of the radiation received by the satellite and the normal to the satellite. This approximation is similar to the one made by Levin (1962), but concerns the radiation received by the satellite rather than that received by a surface element of the Earth.

The above models were analytical or semi-analytical. Even in simplified models, such as those of Lautman (1977a, 1977b), the resulting expressions are complicated. Given the inherent complexity of the problem, other authors have adopted a numerical approach in which the effective portion of the planet is divided into a number of elements whose effects are then summed (McCarthy and Martin, 1977, Knocke and Ries, 1987).

3. Basic equation for the planetary radiation pressure on a spherical satellite

The goal of this section is to derive the basic equation giving the acceleration on a spherical satellite due to solar radiation reflected by an element of planetary surface. To achieve this goal, we first review some fundamental concepts of radiometry, then derive the equation giving the force on a surface element of a satellite due to radiation from a source seen with a small solid angle.

3. 1. FUNDAMENTALS CONCEPTS OF RADIOMETRY

Consider a radiation of given frequency range, falling on an element of surface dS, within a solid angle $d\Omega$ around the unit vector $\hat{u}$. Let $\hat{n}$ be the unit vector along the normal to dS, and θ be the angle between $\hat{u}$ and $\hat{n}$ (see figure 1). We review the concepts of flux of energy and flux of momentum of the radiation.

3. 1. 1. FLUX OF ENERGY AND RADIANCE

(i) Definition. The flux of energy— that is to say the rate of change of the energy per unit area—through dS is

$$dF = L \, d\Omega \, \cos\theta, \tag{1}$$

where L is the radiance of the radiation.

(ii) Examples. A particular case of energy flux is the solar constant. The solar constant is defined as the flux of solar energy which falls *perpendicularly* on an element of surface at the distance $d_0 = 1\text{AU}$. Its value is

$$\Phi_0 = 1367 \text{ W m}^{-2}. \tag{2}$$

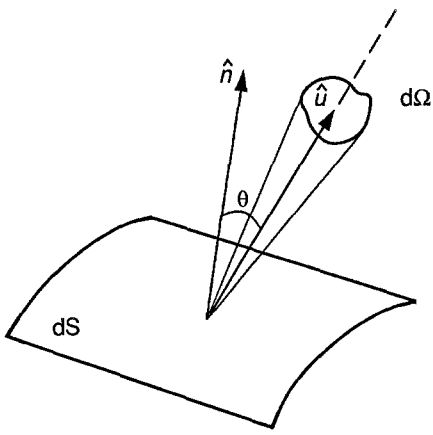

Fig. 1. Geometry for incident rays.

From the conservation of energy, the solar constant at a distance d is

$$\Phi = \frac{\Phi_0}{(d/d_0)^2}. \tag{3}$$

From the definition of the solar constant, it follows that the flux of energy received by an element of planetary surface at the distance d from the Sun, and zenith angle angle ψ_s, is $\Phi \cos\psi_s$. If $\mathcal{A}$ is the albedo of this element of surface, the flux reflected by dS is

$$F = \mathcal{A}\Phi \cos\psi_s. \tag{4}$$

Let us assume that the body satisfies Lambert's law, which means that the reflection is emitted with the same radiance L in all directions over one side of dS. The total flux reflected by dS is

$$F = \int L \, d\Omega \, \cos\theta = \pi \, L. \tag{5}$$

By comparing equations (4) and (5), we find that the radiance of the light diffused by the element of surface of the planet is

$$L = \frac{\mathcal{A}\Phi \cos\psi_s}{\pi}. \tag{6}$$

3. 1. 2. FLUX OF MOMENTUM

(i) Definition. Since the momentum of a photon is equal to its energy divided by the speed of light, the flux vector of momentum through dS is

$$\overrightarrow{d\mathcal{F}} = -\frac{dF}{c} \, \hat{u} = -\frac{L \, d\Omega}{c} \, \cos\theta \, \hat{u}. \tag{7}$$

(ii) Example. If radiation is emitted diffusively from one side of dS, the total flux vector is

$$\vec{\mathcal{F}} = -\int \frac{L\, d\Omega}{c} \cos^2\theta\, \hat{n} = -\frac{2}{3}\frac{\pi L}{c}\, \hat{n}. \tag{8}$$

3. 2. FORCE ON A SURFACE ELEMENT OF A SATELLITE, DUE TO RADIATION FROM A SOURCE SEEN WITH A SMALL SOLID ANGLE

We consider a surface element dS of a spacecraft exposed to incident radiation with radiance L, within the solid angle $d\Omega$ around the unit vector $\hat{u}$. We denote by $\hat{n}$ the unit vector along the normal to dS, and θ the angle between $\hat{u}$ and $\hat{n}$.

The force exerted on dS is proportional to the total momentum flux vector through dS, which, in turn, depends on certain physical properties of dS.

3. 2. 1. PHYSICAL PARAMETERS

Two parameters characterize the reflective properties of dS. They are the total reflectivity, γ, and the specular reflectivity, $\beta\gamma$; γ is the fraction of the incoming flux of energy which is reflected or diffused; β is the fraction of the reflected flux.

The surface element absorbs and reradiates a fraction $\kappa(1-\gamma)$ of the incident flux of energy. Note that the thermal radiation can be taken into account in this model only if its occurs instantaneously. This is what we will assume here. But if the thermal response of dS is not instantaneous, then we must put $\kappa = 0$ in the equations which we are going to derive, and consider the thermal radiation separately.

3. 2. 2. FLUXES THROUGH dS

(i) Incident radiation. From equation (7), the flux of momentum through dS due to the incident radiation is

$$\vec{\mathcal{F}}_i = -\frac{L\, d\Omega}{c} \cos\theta\, \hat{u}. \tag{9}$$

From equation (1), the corresponding flux of energy is

$$F_i = L\, d\Omega\, \cos\theta. \tag{10}$$

(ii) Radiation reflected specularly. Similarly, the flux of momentum through dS due to the radiation reflected specularly is

$$\vec{\mathcal{F}}_s = -\frac{L_s\, d\Omega}{c} \cos\theta\, \hat{v}, \tag{11}$$

where L_s is the radiance of the reflected radiation, and $\hat{v}$ is the unit vector in the direction of propagation of the reflected ray. The corresponding flux of energy is

$$F_s = L_s \, d\Omega \, \cos\theta. \tag{12}$$

Since $\beta\gamma$ is the specular reflectivity, we must have

$$F_s = \beta\gamma F_i, \tag{13}$$

which implies

$$L_s = \beta\gamma L. \tag{14}$$

By substituting equation (14) into equation (11), we obtain

$$\vec{\mathcal{F}}_s = -\beta\gamma \frac{L \, d\Omega}{c} \, \cos\theta \, \hat{v}. \tag{15}$$

(iii) Radiation reflected diffusively. Using the same scaling method as above, we find that the flux of momentum through dS due to the radiation reflected diffusively is

$$\vec{\mathcal{F}}_d = -\frac{2}{3}(1-\beta)\gamma \frac{L \, d\Omega}{c} \cos\theta \, \hat{n}, \tag{16}$$

(iv) Thermal radiation. Similarly, the flux of momentum through dS due to the thermal radiation is

$$\vec{\mathcal{F}}_t = -\frac{2}{3}\kappa(1-\gamma) \frac{L \, d\Omega}{c} \cos\theta \, \hat{n}. \tag{17}$$

(v) Total flux. Using equations (9), (15), (16), and (17), we obtain the total flux, which we write in the form

$$\vec{\mathcal{F}} = -\frac{L \, d\Omega}{c} \cos\theta \left[(1-2\mu)\hat{u} + (2\nu + 4\mu\cos\theta)\hat{n}\right], \tag{18}$$

with

$$\mu = \frac{1}{2}\beta\gamma, \tag{19}$$

and

$$\nu = \frac{1}{3}\left[\gamma(1-\beta) + \kappa(1-\gamma)\right]. \tag{20}$$

3. 2. 3. FORCE EXERTED ON dS

The force exerted on dS is

$$\vec{\mathbf{F}} = -\frac{L \, d\Omega}{c} \cos\theta \, dS \left[(1-2\mu)\hat{u} + (2\nu + 4\mu\cos\theta)\hat{n}\right]. \tag{21}$$

3. 3. ELEMENTARY ACCELERATION OF A SPHERICAL SATELLITE DUE TO PLANETARY RADIATION PRESSURE

We integrate equation (21) over the surface of the satellite in order to find the force exerted on a spherical satellite. Then we specialize this result to the case where the incident radiation consists of solar radiation reflected by a surface element of a planet.

3. 3. 1. FORCE ON A SPHERICAL SATELLITE

To compute the force exerted on a spherical satellite of radius s, we integrate the elementary force, as given by equation (21) over one hemisphere. We obtain

$$\overrightarrow{\mathbf{F}} = -k\pi s^2 \frac{L\ d\Omega}{c}\hat{u}, \tag{22}$$

with

$$k = 1 + \frac{4}{3}\nu. \tag{23}$$

Let M be the mass of the satellite. The acceleration exerted on the satellite is

$$\overrightarrow{\Gamma} = -k\frac{\pi s^2}{M}\frac{L\ d\Omega}{c}\hat{u}. \tag{24}$$

3. 3. 2. CASE WHERE THE INCIDENT RADIATION CONSISTS OF SOLAR LIGHT REFLECTED BY A SURFACE ELEMENT OF A PLANET

Consider a spherical satellite with center C struck by radiation diffused by an element of surface $d\sigma$ around a point P of the planetary surface. The solid angle $d\Omega$ of the incomming radiation is

$$d\Omega = \frac{\cos\psi\ d\sigma}{D^2}, \tag{25}$$

where ψ is the satellite zenith angle (see figure 2), and

$$D = |\overrightarrow{PC}|. \tag{26}$$

We substitute equation (25) and equation (6) for the radiance of the radiation into equation (24). We obtain

$$\overrightarrow{\Gamma} = k\frac{s^2}{M}\mathcal{A}\frac{\Phi}{c}\ \frac{\cos\psi_s\ \cos\psi\ d\sigma}{D^3}\overrightarrow{\mathrm{PC}}. \tag{27}$$

4. Model

First, we describe the particular representation for the locations of the contributing points on the planetary surface, assumed to be spherical. Our choice of variables yields the simplest limits of integration. The inner integrals in the expressions for the acceleration components are readily computed, so that the acceleration components are expressed in terms of one-dimensional integrals. These integrals can be computed analytically in the case where the spacecraft does not "see" the terminator. We also calculated analytically approximate expressions for the other integrals, and compared the results of this model with those obtained by Lochry (1966). Finally, we give the equations to compute the acceleration components in the orbital reference frame.

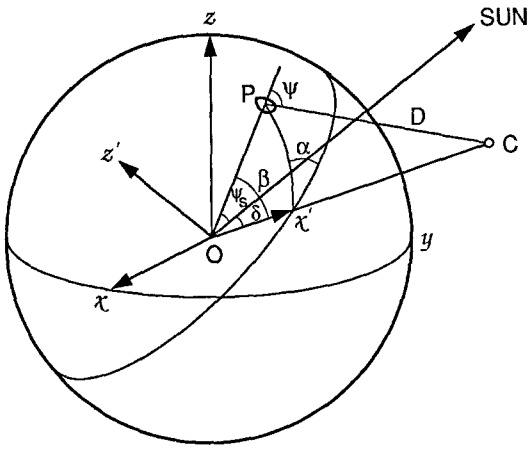

Fig. 2. Geometry for the model of planetary radiation pressure.

4. 1. CHOICE OF COORDINATE AXES AND VARIABLES

The choice of the coordinate axes and variables is motivated by the following considerations. The cap of the planet visible to the satellite is limited by a circle whose axis of symmetry is OC, the center of the planet-satellite direction (see figure 2). The points on this cap can be viewed as belonging to circles whose distance from their axis of symmetry OC is characterized by the angle β (note here the change of meaning from the parameter β of section 3.2.1.). The position of a point on one of these circle is characterized by the angle α. Each circle is completely on the day side of the planet, or completely on the night side, or partly in the day, partly in the night. In that case the slice of circle which is in the day is symmetric with respect to the plane defined by the Sun, the satellite and the center of the planet. One can expect that the best reference frame has this plane as a plane of reference, and the direction of the satellite as an axis.

Consequently, we work in the rectangular, right-handed reference frame $Ox'y'z'$ such that Ox' is in the direction of the satellite, and Oz' is normal to the plane

containing the center of the Earth O, the satellite C, and the Sun. The precise definition of the $Ox'y'z'$ system of coordinate axes is as follows.

Let $\overrightarrow{U'}$, $\overrightarrow{V'}$, and $\overrightarrow{W'}$ be the unit vectors along the axes Ox', Oy', and Oz', respectively (see figure 2). $\overrightarrow{U'}$ is the unit vector from the center of the planet to the center of the spacecraft. Let $\overrightarrow{U}_{\odot}$ be the unit vector in the center of the planet-Sun direction. Let δ be the angle between $\overrightarrow{U'}$ and $\overrightarrow{U}_{\odot}$, that is to say the phase angle of the spacecraft (the angle from the center of the planet between the spacecraft and the Sun). The vector $\overrightarrow{V'}$ is defined by the conditions

$$\overrightarrow{V'} = a\overrightarrow{U'} + b\overrightarrow{U}_{\odot}, \tag{28}$$

$$| \overrightarrow{V'} | = \sqrt{a^2 + b^2 + 2ab\overrightarrow{U'} \cdot \overrightarrow{U}_{\odot}} = 1, \tag{29}$$

$$\overrightarrow{U'} \cdot \overrightarrow{V'} = a + b\overrightarrow{U'} \cdot \overrightarrow{U}_{\odot} = 0, \tag{30}$$

and

$$\overrightarrow{U}_{\odot} \cdot \overrightarrow{V'} > 0. \tag{31}$$

These conditions imply

$$\overrightarrow{V'} = \frac{1}{\sin\delta}\left(-\cos\delta\ \overrightarrow{U'} + \overrightarrow{U}_{\odot}\right). \tag{32}$$

Finally, the vector $\overrightarrow{W'}$ is defined by

$$\overrightarrow{W'} = \overrightarrow{U'} \times \overrightarrow{V'}. \tag{33}$$

Next, we evaluate the quantities in equation (27). The components of the vector $\overrightarrow{PC}$ in the $Ox'y'z'$ reference frame are

$$\overrightarrow{PC} \left| \begin{array}{l} r - R\cos\beta \\ -R\sin\beta\cos\alpha \\ -R\sin\beta\sin\alpha \end{array} \right. \quad Ox'y'z' \tag{34}$$

where r is the orbital radius, and R is the radius of the planet. We have also

$$\cos\psi_s = \cos\delta\cos\beta + \sin\delta\sin\beta\cos\alpha, \tag{35}$$

$$\cos\psi = \frac{r\cos\beta - R}{D}, \tag{36}$$

$$D = \left(r^2 + R^2 - 2rR\cos\beta\right)^{1/2}, \tag{37}$$

$$d\sigma = R^2 \sin\beta \; d\beta \; d\alpha. \tag{38}$$

We define

$$\xi = \frac{R}{r}. \tag{39}$$

4. 2. LIMITS OF INTEGRATION

The limits of integration with respect to β are given by $0 \leq \beta \leq \beta_\ell$ with $\cos\beta_\ell = \xi$ and $0 \leq \beta_\ell \leq \frac{\pi}{2}$.

The limits of integration with respect to α are given by $-\alpha_\ell \leq \alpha \leq \alpha_\ell$ with $\alpha_\ell \geq 0$ and

- ⋆ If $0 \leq \delta \leq \frac{\pi}{2} - \beta$, $\alpha_\ell = \pi$ (the cap visible to the satellite is in the day).
- ⋆ If $\frac{\pi}{2} - \beta \leq \delta \leq \frac{\pi}{2} + \beta$, $\cos\alpha_\ell = -\cot\beta\cot\delta$ (the cap visible to the satellite is partially in the day, partially in the night).
- ⋆ If $\delta \geq \frac{\pi}{2} + \beta$, $\alpha_\ell = 0$ (the cap visible to the satellite is in the night).

4. 3. COMPONENTS OF THE ACCELERATION

We substitute equations (34) to (39) into equation (27), then write the integral of the elementary force over the effective portion of the Earth, and perform analytically the integration with respect to α. We find that the component of the acceleration along the Oz' axis cancels. The two other components, $\Gamma_{x'}$ and $\Gamma_{y'}$, are written in the form

$$\Gamma_{x'} = k\frac{s^2}{M}\mathcal{A}\frac{\Phi}{c}\xi^2 J_{x'}, \tag{40}$$

and

$$\Gamma_{y'} = -k\frac{s^2}{M}\mathcal{A}\frac{\Phi}{c}\xi^3 J_{y'}. \tag{41}$$

The quantities $J_{x'}(\xi,\delta)$ and $J_{y'}(\xi,\delta)$ are given below.

4. 3. 1. COMPONENT ALONG Ox' (RADIAL COMPONENT)

First case of illumination : $\delta < \pi/2$ and $\sin\delta \leq \xi$

$$\begin{aligned} J_{x'} &= 2\pi\cos\delta \int_0^{\beta_\ell} d\beta \frac{\sin\beta(\cos\beta - \xi)(1 - \xi\cos\beta)\cos\beta}{\left(1 - 2\xi\cos\beta + \xi^2\right)^2} \\ &= \frac{\pi}{4}\frac{\cos\delta}{\xi^2}\left[1 + \xi^2 + 2\xi^3 - \frac{(1-\xi^2)^2}{2\xi}\log\left(\frac{1+\xi}{1-\xi}\right)\right] \end{aligned} \tag{42}$$

Second case of illumination : $\delta < \pi/2$ *and* $\sin\delta > \xi$

$$J_{x'} = 2\pi\cos\delta\left[F\left(\frac{\pi}{2}-\delta\right)-F(0)\right]$$

$$+2\int_{\frac{\pi}{2}-\delta}^{\beta_\ell} d\beta \frac{\sin\beta(\cos\beta-\xi)(1-\xi\cos\beta)}{(1-2\xi\cos\beta+\xi^2)^2}\left[\alpha_\ell\cos\delta\cos\beta+\sin\delta\sin\beta\sin\alpha_\ell\right] \tag{43}$$

The function F is defined in 4. 3. 3.

Third case of illumination : $\delta \geq \pi/2$ *and* $\sin\delta > \xi$

$$J_{x'} = 2\int_{-\frac{\pi}{2}+\delta}^{\beta_\ell} d\beta \frac{\sin\beta(\cos\beta-\xi)(1-\xi\cos\beta)}{(1-2\xi\cos\beta+\xi^2)^2}\left[\alpha_\ell\cos\delta\cos\beta+\sin\delta\sin\beta\sin\alpha_\ell\right] \tag{44}$$

Fourth case of illumination : $\delta \geq \pi/2$ *and* $\sin\delta \leq \xi$

$$J_{x'} = 0 \tag{45}$$

4. 3. 2. COMPONENT ALONG Oy' (PSEUDO-TRANSVERSE COMPONENT)

First case of illumination : $\delta < \pi/2$ *and* $\sin\delta \leq \xi$

$$J_{y'} = \pi\sin\delta\int_0^{\beta_\ell} d\beta \frac{\sin^3\beta(\cos\beta-\xi)}{(1-2\xi\cos\beta+\xi^2)^2}$$

$$= -\frac{\pi}{8}\sin\delta\frac{(1-\xi)}{\xi^3}\left[3+3\xi+2\xi^2-\frac{(3+\xi^2)(1+\xi)}{2\xi}\log\left(\frac{1+\xi}{1-\xi}\right)\right] \tag{46}$$

Second case of illumination : $\delta < \pi/2$ *and* $\sin\delta > \xi$

$$J_{y'} = \pi\sin\delta\left[G\left(\frac{\pi}{2}-\delta\right)-G(0)\right]+\int_{\frac{\pi}{2}-\delta}^{\beta_\ell} d\beta\frac{\sin^2\beta(\cos\beta-\xi)}{(1-2\xi\cos\beta+\xi^2)^2}\times$$

$$\left[2\cos\delta\cos\beta\sin\alpha_\ell+\alpha_\ell\sin\delta\sin\beta+\frac{1}{2}\sin\delta\sin\beta\sin 2\alpha_\ell\right] \tag{47}$$

The function G is defined in 4. 3. 3.

Third case of illumination : $\delta \geq \pi/2$ *and* $\sin\delta > \xi$

$$J_{y'} = \int_{-\frac{\pi}{2}+\delta}^{\beta_\ell} d\beta \frac{\sin^2\beta(\cos\beta - \xi)}{(1 - 2\xi\cos\beta + \xi^2)^2} \times \tag{48}$$

$$\left[2\cos\delta\cos\beta\sin\alpha_\ell + \alpha_\ell \sin\delta\sin\beta + \frac{1}{2}\sin\delta\sin\beta\sin 2\alpha_\ell\right]$$

Fourth case of illumination : $\delta \geq \pi/2$ *and* $\sin\delta \leq \xi$

$$J_{y'} = 0 \tag{49}$$

4. 3. 3. DEFINITION OF THE FUNCTIONS F AND G

The functions F and G appearing explicitely in equations (43) and (47), respectively, and implicitely in equations (42) and (46), are defined by

$$F(\beta) = \int^{\beta} d\beta \frac{\sin\beta(\cos\beta - \xi)(1 - \xi\cos\beta)\cos\beta}{(1 - 2\xi\cos\beta + \xi^2)^2} \tag{50}$$

$$= \frac{1}{4\xi}\left[\frac{X^2}{2} + x_0 X - x_1^2 \log \mid X \mid + \frac{x_1^2 x_0}{X}\right]$$

and

$$G(\beta) = \int^{\beta} d\beta \frac{\sin^3\beta(\cos\beta - \xi)}{(1 - 2\xi\cos\beta + \xi^2)^2} \tag{51}$$

$$= \frac{1}{4\xi^2}\left[\frac{X^2}{2} + (2x_0 + x_1)X + x_1(2x_0 + x_1)\log \mid X \mid - \frac{x_1^3}{X}\right]$$

with

$$x_0 = \frac{1 + \xi^2}{2\xi}, \tag{52}$$

$$x_1 = \frac{1 - \xi^2}{2\xi}, \tag{53}$$

and

$$X = \cos\beta - x_0. \tag{54}$$

In the first case of illumination, and in the limit where ξ is small, we have

$$\Gamma_{x'} = \pi k \frac{s^2}{M}\mathcal{A}\frac{\Phi}{c}\xi^2\cos\delta\left[\frac{2}{3} + \frac{1}{2}\xi - \frac{2}{15}\xi^2 - \frac{1}{105}\xi^4 + \ldots\right], \tag{55}$$

and

$$\Gamma_{y'} = -\pi k \frac{s^2}{M} \mathcal{A} \frac{\Phi}{c} \xi^3 \sin\delta \left[\frac{1}{4} - \frac{2}{15}\xi - \frac{4}{105}\xi^3 + \dots \right]. \tag{56}$$

In the limit where $\xi \to 1$, we have $F(\beta_\ell) - F(0) \to 1/2$ and

$$\Gamma_{x'} \to \pi k \frac{s^2}{M} \mathcal{A} \frac{\Phi}{c} \xi^2 \cos\delta, \tag{57}$$

while $G(\beta_\ell) - G(0) \to 0$ and

$$\Gamma_{y'} \to 0. \tag{58}$$

4. 4. APPROXIMATE ANALYTICAL SOLUTION FOR A DISTANT SATELLITE

We wrote equations (42) to (49) to the lowest order in ξ and integrated them analytically. The calculations are very complicated. We obtained the same results by a simpler method which consists in using, instead of the variables α and β, the spherical coordinates with respect to $Ox'y'z'$. To the lowest order in ξ, one can assume that the satellite sees one hemisphere of the planet, while the Sun lights another hemisphere. These assumptions make the limits of integration particularly simple and independent. Note, however, that this method is more complicated at the next order of approximation. As a matter of fact, both variables of integration appears in D rather than one. The results are

Case where $\delta \leq \pi/2 - \beta_\ell$

$$\Gamma_{x'} = \frac{2\pi}{3} k \frac{s^2}{M} \mathcal{A} \frac{\Phi}{c} \xi^2 \cos\delta \tag{59}$$

$$\Gamma_{y'} = -\frac{\pi}{4} k \frac{s^2}{M} \mathcal{A} \frac{\Phi}{c} \xi^3 \sin\delta \tag{60}$$

Case where $\pi/2 - \beta_\ell < \delta < \pi/2 + \beta_\ell$

$$\Gamma_{x'} = \frac{2}{3} k \frac{s^2}{M} \mathcal{A} \frac{\Phi}{c} \xi^2 \left[(\pi - \delta)\cos\delta + \sin\delta \right] \tag{61}$$

$$\Gamma_{y'} = -\frac{\pi}{8} k \frac{s^2}{M} \mathcal{A} \frac{\Phi}{c} \xi^3 \sin\delta (1 + \cos\delta) \tag{62}$$

Case where $\pi/2 + \beta_\ell \leq \delta$

$$\Gamma_{x'} = 0 \tag{63}$$

$$\Gamma_{y'} = 0 \tag{64}$$

4. 5. COMPARISON WITH THE RESULTS OF LOCHRY

Lochry (1966) computed an analytical solution in power of ξ. His equations when the spacecraft does not see the terminator are the same as those of our approximate solution, as given in equations (55) and (56). Moreover, from his work (pages 63 and 167), we should have for the cases 2 and 3 of illumination :

$$J_{x'} = \frac{2}{3}\left[(\pi - \delta)\cos\delta + \sin\delta\right] + \frac{\pi}{8}\xi\left(2\cos\delta + 2 - 3\sin^2\delta\right) -$$

$$\frac{1}{15}\xi^2\left[2(\pi - \delta)\cos\delta - 13\sin\delta + 16\sin^3\delta\right] + \frac{\pi}{12}\xi^3\left(-2 + 7\sin^2\delta - 5\sin^4\delta\right), \tag{65}$$

$$J_{y'} = \frac{\pi}{8}(1 + \cos\delta)\sin\delta - \frac{2}{15}\xi\left[(\pi - \delta)\sin\delta - 4\cos\delta\sin^2\delta\right] - \frac{\pi}{4}\xi^2\sin\delta\cos^3\delta -$$

$$\frac{4}{105}\xi^3\left[(\pi - \delta)\sin\delta + \cos\delta\left(-8 + 36\sin^2\delta + 32\sin^4\delta\right)\right] +$$

$$\frac{\pi}{48}\xi^4\cos\delta\left(10\sin\delta + 40\sin^3\delta + 30\sin^5\delta\right) \tag{66}$$

Actually, Lochry gives terms up to order ξ^6 for the equation corresponding to $J_{x'}$, but, as will be seen below, equation (65) is already precise enough. As for $J_{y'}$, Lochry gives one more term, of order ξ^5, but which cannot be used due to a typographic error. Values of $J_{x'}$ and $J_{y'}$ computed by the two methods are shown in figures 3 and 4. The agreement between the exact calculation and the analytical approximation is good for $J_{x'}$ but not for $J_{y'}$, possibly indicating that there is an error in Lochry's approximate formula for $J_{y'}$, or simply a problem of convergence.

Because of the disagreement between our results and those of Lochry for $J_{y'}$, we did not use his analytical expressions. Instead, we made a table of the integrals on a grid of points (ξ, δ) and computed $J_{x'}$ and $J_{y'}$ at any point by interpolation.

4. 6. COMPONENTS OF THE FORCE IN THE ORBITAL FRAME

Let $\vec{U}$, $\vec{V}$, and $\vec{W}$, be the unit vectors along the axes of the orbital reference frame. These vectors define a right-handed, rectangular system of coordinate axes. The vector $\vec{U} = \vec{U'}$, the vector $\vec{W}$ is directed along the orbital momentum vector.

The components of the acceleration in the orbital reference frame are given by

$$\Gamma_r = \Gamma_{x'}, \tag{67}$$

$$\Gamma_t = \frac{\vec{U}_\odot \cdot \vec{V}}{\sin\delta}\,\Gamma_{y'}, \tag{68}$$

and

$$\Gamma_n = \frac{\vec{U}_\odot \cdot \vec{W}}{\sin\delta}\,\Gamma_{y'}. \tag{69}$$

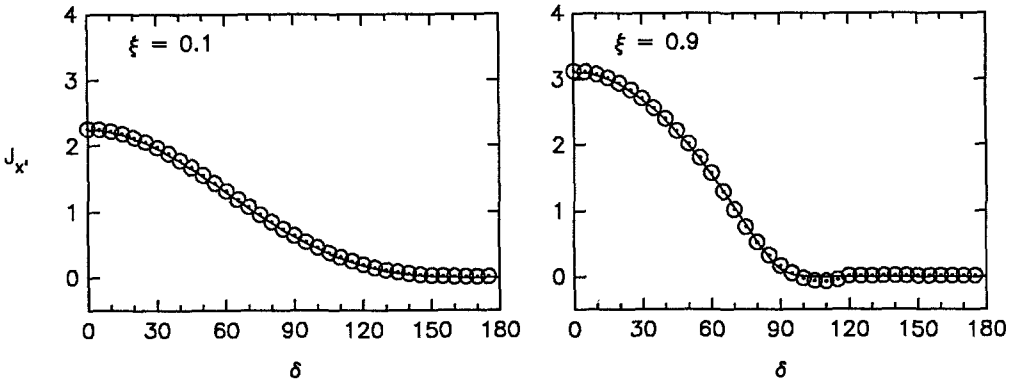

Fig. 3. Plots of $J_{x'}$ as functions of the phase angle δ for $\xi = 0.1$ and 0.9. The solid line represents the solution obtained from the numerical quadrature while the dotted circles correspond to the analytical calculations (our exact calculation in the first case of illumination, approximate equations (65) and (66) from Lochry in the second and third cases of illumination).

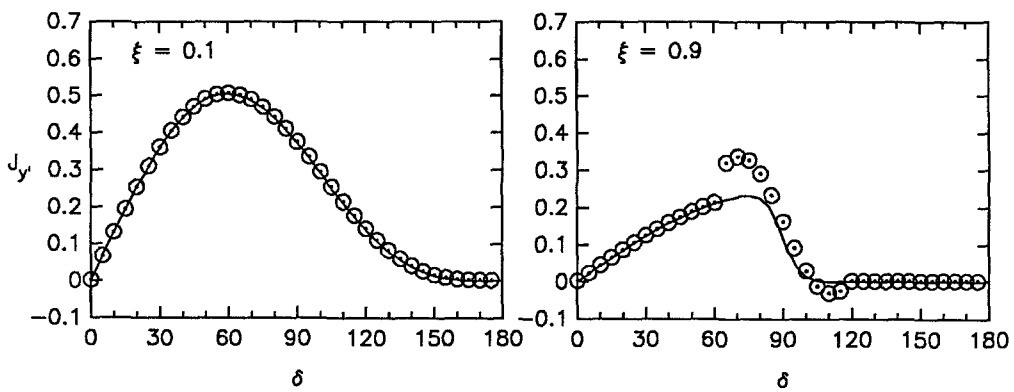

Fig. 4. Same as Fig. 3., but for $J_{y'}$.

5. Application to Magellan

We studied the albedo radiation pressure on a Venus'orbiter moving on the nominal orbit of Magellan, as well as on a similar orbit but with a small eccentricity. Since we assumed that the spacecraft was spherical, which is not true of Magellan, this

study is intended as an illustration of the albedo radiation pressure effects, rather than a precise evaluation of these effects on Magellan. In both cases, we integrated numerically the equations of motion. The initial conditions and physical parameters are given below. We examined the conditions of illumination and the acceleration components for the circular and eccentric orbits, and computed the variations of the elements for the nominal orbit.

5. 1. NUMERICAL INTEGRATION

The numerical integration of the equations of motion was performed in osculating elements—the semi-major axis, a, the eccentricity, e, the inclination I, the longitude of the node, Ω, the argument of periapse, ω, and the mean anomaly, M—with respect to the reference frame VME85 defined by the planet equator and its ascending node on the Earth equator. At the initial time of the integration, August 10, 1990, 16 hr, 40 mn, the orbital elements were :

$a = 10190.3$ km,
$e = 0.38$,
$I = 85°.3$,
$\Omega = -62°.3$,
$\omega = 170°$,
$M = 0°$,

This target orbit for the first periapse passage has a a periapse altitude of 275 km, and a period of 3.15 hr. Most of the results presented below have been obtained through a 7 hr numerical integration, hence covering more than 2 orbits. We characterize the results obtained with these initial conditions by the label "case b". We also used initial orbital elements similar to those given above, except that the eccentricity was changed from 0.38 to 0.001 ("case a").

For the coefficient of reflectivity k, defined by equation (23), we chose arbitrarily an average value of 1.2. The cross section was $\pi s^2 = 14$ m^2, which is about right for Magellan. The spacecraft mass was 1100 kg, the mass of Magellan at insertion in orbit around Venus. The solar constant at Venus is 2621 W m^{-2} and the albedo of Venus is 0.76 (Taylor *et al.*, 1983).

5. 2. GEOMETRY AND CONDITIONS OF ILLUMINATIONS

A qualitative understanding of the geometry can be obtained by thinking of Magellan's orbit as polar, and of the Sun as located in the equatorial plane of Venus with longitude $\lambda_\odot \simeq -90°$ at the initial time of the integration. With these two approximations, we have $\cos\delta = \cos(\lambda_\odot - \Omega)\cos(\omega + f) \simeq \cos(30°)\cos(170° + f)$. This behavior of the phase angle is indeed found in figure 5. In the case of the low eccentricity orbit, δ is nearly a sinusoidal function of the time, while in the case of the eccentric orbit, the curve representing $\delta(t)$ is flatter around the times corresponding to apoapse passages.

Figures 6a and 6b, showing the plots of ξ and $\sin\delta$ as a function of time, allow one, together with figures 5a and 5b, to determine the conditions of illumination

in both cases.

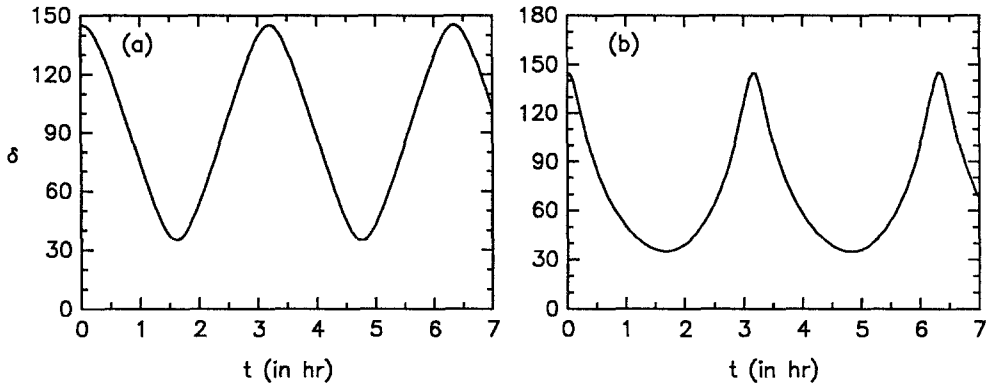

Fig. 5. Plots of the phase angle δ between the spacecraft and the Sun directions from the center of Venus, for the initial conditions described in subsection 5.1. corresponding to the cases where the orbit of the spacecraft is nearly circular (a), or elliptical (b).

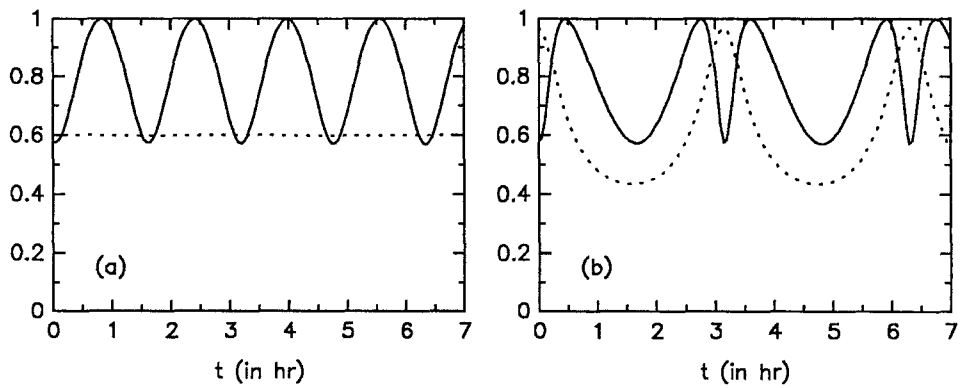

Fig. 6. Plots of $\sin\delta$ (solid line) and of $\xi = R/r$, the ratio of the planet radius to the spacecraft orbital radius, (dotted line), in the cases of a nearly circular (a) or elliptical (b) orbits.

Remember that the conditions of illumination can be characterized as follows :

1. If $\sin\delta > \xi$, then the spacecraft sees a planetary cap which is partially illuminated.
2. If $\sin\delta \leq \xi$ and $\delta < \pi/2$, then the cap seen by the spacecraft is completely illuminated.
3. If $\sin\delta \leq \xi$ and $\delta \geq \pi/2$, then the cap seen by the spacecraft is entirely in the dark.

From figures 5a and 6a, we see that in case a, the Venusian cap visible to the spacecraft is most of the time partially illuminated, although during brief intervals

of time around the passages of δ through maximum or minimum values, the cap is totally in the dark or totally illuminated, respectively. This geometry is modified in case b : the cap visible to the satellite is still in the dark around the times where δ is maximum, and these interval of times are longer than in the circular case; on the other hand, the cap is never totally illuminated, because when δ is minimum the spacecraft is at apoapse and sees more of the planet than in the circular case.

5. 3. ACCELERATIONS

We examine the radial, pseudo-transverse, transverse, and normal components of the acceleration scaled to n^2a : $\gamma_{x'} = \Gamma_{x'}/n^2a$, $\gamma_{y'} = \Gamma_{y'}/n^2a$, $\gamma_t = \Gamma_t/n^2a$, and $\gamma_n = \Gamma_n/n^2a$.

5. 3. 1. RADIAL COMPONENT

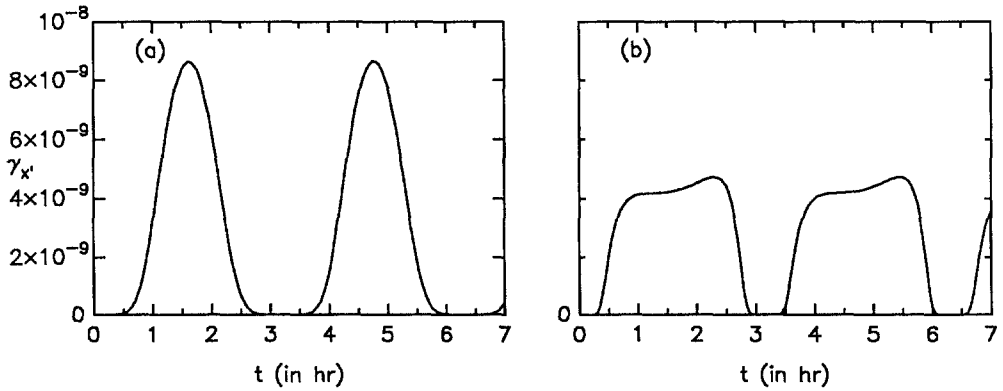

Fig. 7. Plots of $\gamma_{x'} = \Gamma_{x'}/(n^2a)$ in the cases of a nearly circular (a) or elliptical (b) orbits. The vertical scale is the same in both plots.

Let us first examine the radial component $\gamma_{x'}$, shown on figure 7. We can make three comments :

1. $\gamma_{x'} > 0$, in agreement with the fact that the radiation pressure always pushes the spacecraft away from the source of radiation, which here is the planet.
2. In case a, $\gamma_{x'}$ is in opposition of phase with δ, reflecting the fact that the acceleration is maximum when the illumination of the cap visible to the satellite is maximum, that is to say when δ is minimum, and vice-versa. In case b, this behavior is modified by the orbital eccentricity, which shifts the maximum of $\gamma_{x'}$ with respect to the minimum of δ. Because the maximum of illumination of the cap occurs when the spacecraft is near apoapse, the acceleration reaches a smaller maximum value in case b compared to case a. If, on the contrary, the maximum of illumination of the cap occured when the spacecraft is near periapse, the maximum value of $\gamma_{x'}$ would be greater than in the circular case.

3. In case a, the curve representing the variations of $\gamma_{x'}$ as a function of time is flatter at its minimum than at its maximum. This behavior can be understood by looking at figure 8. As seen from equation (27), the acceleration produced by an element of surface around a point P of the cap is proportional to $\cos\psi \cos\psi_s$ where ψ is the spacecraft zenith angle, and ψ_s is the solar zenith angle.
   - ⋆ In the case of maximum illumination, illustrated by figure 8.1, most of the contribution to the acceleration comes from a circular portion of the cap around the sub-spacecraft point. As the spacecraft moves around the point where δ is maximum, we have $\cos\psi \approx$ const. $= 1$, while $\cos\psi_s \approx \cos\delta$. It follows that $\gamma_{x'}$ varies approximately as $\cos\delta$.
   - ⋆ In the case of minimum illumination, illustrated by figure 8.2, most of the contribution to the acceleration comes from a circular portion of the cap around a point of its lit part roughly midway between the terminator and the limit of the cap. As the spacecraft moves around the point where δ is minimum, we have $\cos\psi \approx \cos(\delta/2)$, and $\cos\psi_s \approx \cos(\delta/2)$. It follows that $\gamma_{x'}$ varies approximately as $\frac{1}{2}\cos\delta$, which corresponds to a flatter curve.

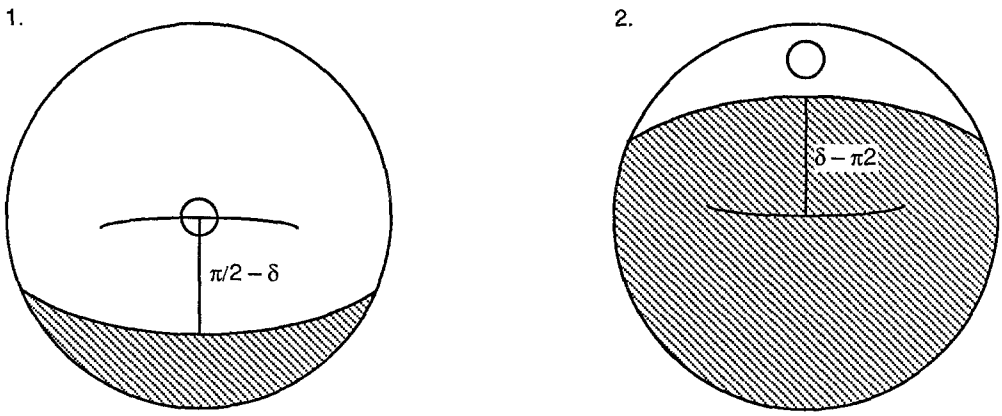

Fig. 8. Schematic view of the portion of planet visible to the spacecraft. The large circle represent the cap seen by the spacecraft, the sub-spacecraft point being in the center of the circle. The Sun direction is along the axis perpendicular to the sheet of paper and passing by the center of the circle. The part of the cap which is in the dark is represented as a shaded area. Figures 8.1 and 8.2 correspond to the case where the illumination is maximum (δ minimum) and minimum (δ maximum), respectively. In both cases the projection of the spacecraft orbit around the sub-spacecraft point is locally parallel to the terminator.

5. 3. 2. PSEUDO-TRANSVERSE COMPONENT

The pseudo-transverse component $\gamma_{y'}$ is shown on figure 9. We can make the two following comments :

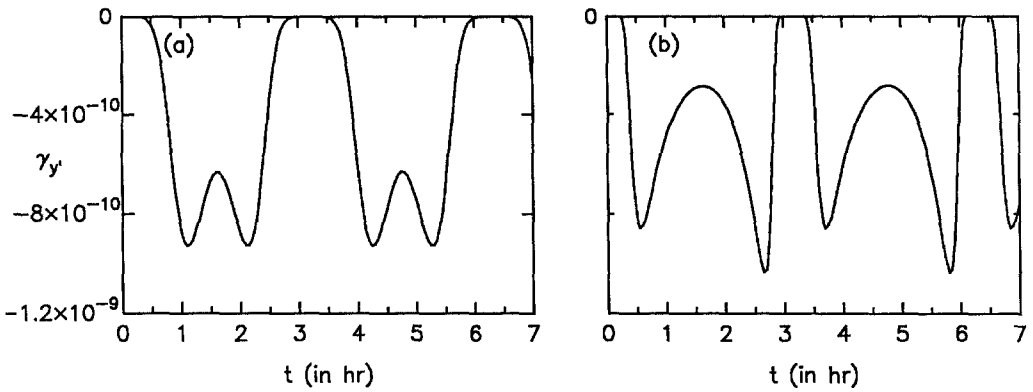

Fig. 9. Plots of $\gamma_{y'} = \Gamma_{y'}/(n^2 a)$ in the cases of a nearly circular (a) or elliptical (b) orbits. The vertical scale is the same on both plots.

1. The magnitude of the pseudo-transverse component of the acceleration is smaller than that of the radial component. This is readily explained by the fact that the contributions of all the elements of the effective area of the planet add for the radial component, while there is a lot of cancellation for the pseudo-transverse component. The local minimum of $\mid \gamma_{y'} \mid$ when the illumination of the cap visible to the satellite is maximum (δ minimum) is due to this effect of cancellation.
2. $\gamma_{y'} < 0$, in agreement with the fact that the radiation pressure always pushes the spacecraft away from the source of radiation, hence toward the terminator.

5. 3. 3. TRANSVERSE COMPONENT

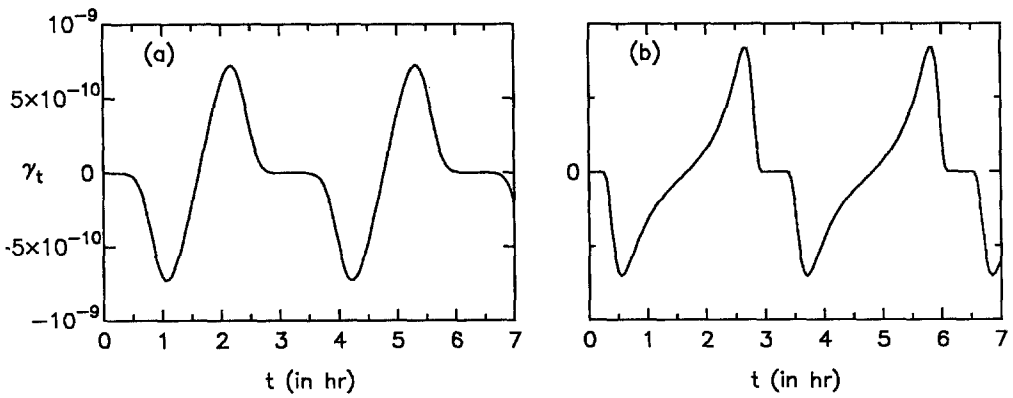

Fig. 10. Plots of $\gamma_t = \Gamma_t/(n^2 a)$ in the cases of a nearly circular (a) or elliptical (b) orbits. The vertical scale is the same on both plots.

The transverse component γ_t is shown on figure 10. We can make three comments :

1. The magnitude of the transverse component is smaller than the magnitude of the radial component, due to an effect of cancellation.
2. The sign of the force can be understood by looking at the figures 11.1 and 11.2. These figures are similar to figures 8.1 and 8.2, except that they are drawn in the case where δ is neither minimum nor maximum. By projecting on the orbit path the total acceleration, which is always directed toward the terminator, we see that in the case illustrated by figure 11.1 where δ is decreasing, $\gamma_t < 0$, while in the case illustrated by figure 11.2 where δ is increasing, $\gamma_t > 0$. We see also that $\gamma_t = 0$ when δ is maximum or minimum.
3. The curve of γ_t around the points where the transverse acceleration is equal to zero if much flatter when δ is maximum than when δ is minimum. This is due to the same cause which explains why the curve of $\gamma_{x'}$ is flatter at δ maximum in case a.

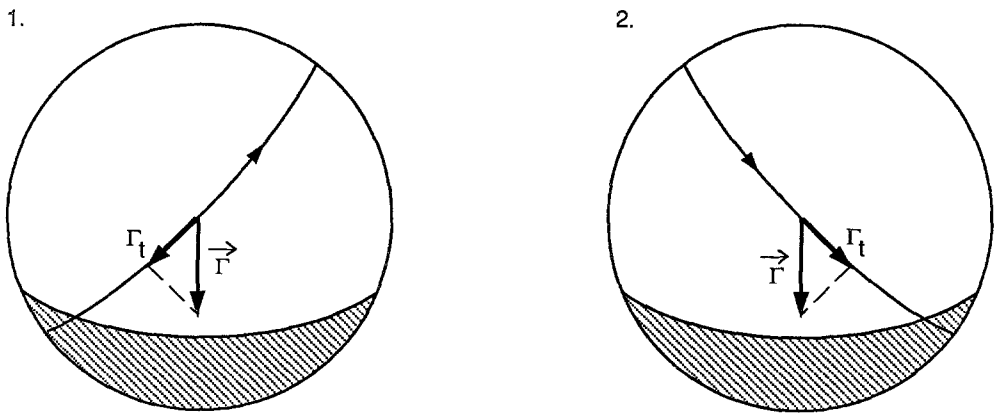

Fig. 11. Similar to figures 8.1 and 8.2, except that δ is neither minimum nor maximum. In figure 11.1, δ is decreasing as the spacecraft is moving on its orbit, while in figure 11.2, δ is increasing.

5. 3. 4. NORMAL COMPONENT

Finally, the normal component γ_n is shown on figure 12.

5. 4. VARIATIONS OF THE ELEMENTS

The variations of a, e, I, Ω, ω, and M due to the Venusian radiation pressure, and corresponding to case b are shown in figure 13. The global decrease in the eccentricity and semi-major axis can be understood as follows. One can think of the radiation pressure force as a radial impulse, directed outward, and exerted when the spacecraft is at apoapse. The spacecraft reaches its periapse farther away from the planet than if the impulse had not been applied, and the eccentricity tends

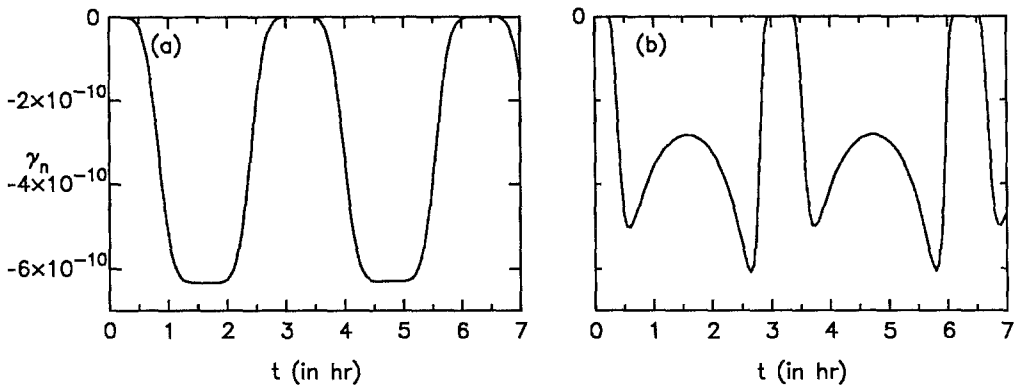

Fig. 12. Plots of $\gamma_n = \Gamma_n/(n^2 a)$ in the cases of a nearly circular (a) or elliptical (b) orbits. The vertical scale is the same on both plots.

to decrease. Moreover, since the acceleration is essentially radial, the angular momentum is nearly conserved, and the semi-major axis also decreases. If, on the contrary, the maximum illumination of the cap visible to the satellite occured when the spacecraft is at periapse, a and e would increase.

If the orientation of the orbit with respect to the Sun did not change this effect would be secular. But, mainly due to the fact that Venus rotates around the Sun (in about 225 days), the geometry changes and gives rise to a long periodic variations of a and e and the other orbital elements. The long term variations of the orbital elements over 225 days are shown on figure 14. One can see that in addition to the long periodic effect, a secular effect is present for most variables. The short periodic variations are enhanced during the interval of time where the cap visible to the spacecraft when the latter is at periapse is well illuminated by the Sun, roughly between the days 80 and 190 of the numerical integration.

6. Summary

The main results of the model can be summarized as follows. The components of the acceleration in the $Ox'y'z'$ coordinate system are given in subsection 4.3. These components are expressed in terms of integrals which depends only on the two parameters δ and ξ, where δ is the angle from the center of the planet between the spacecraft and the Sun directions, and ξ is the ratio of the planet's radius to the orbital radius. In the case where the spacecraft does not "see" the terminator, exact expressions are obtained. In the case where the spacecraft "sees" the terminator, the problem is reduced to the evaluation of one-dimensional integrals. Approximate expressions are given in subsection 4.4. for the case where the satellite is distant ($\xi \ll 1$). The components of the acceleration in the orbital reference frame can be computed using equations (67), (68), and (69) of subsection 4.6.

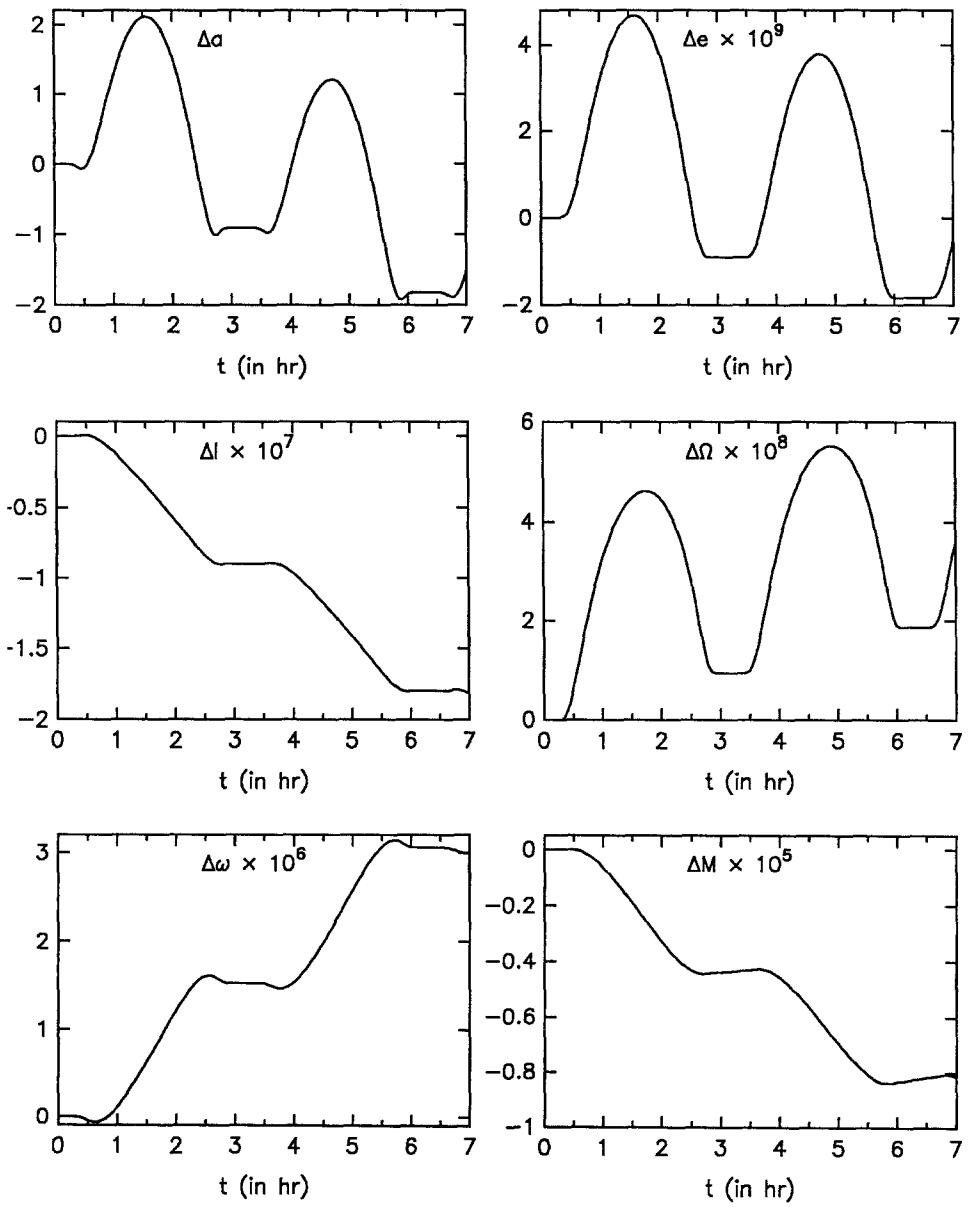

Fig. 13. Variations of a, e, I, Ω, ω and M, due to the Venusian radiation pressure, and corresponding to case b; Δa is in cm, and the angles are in degree.

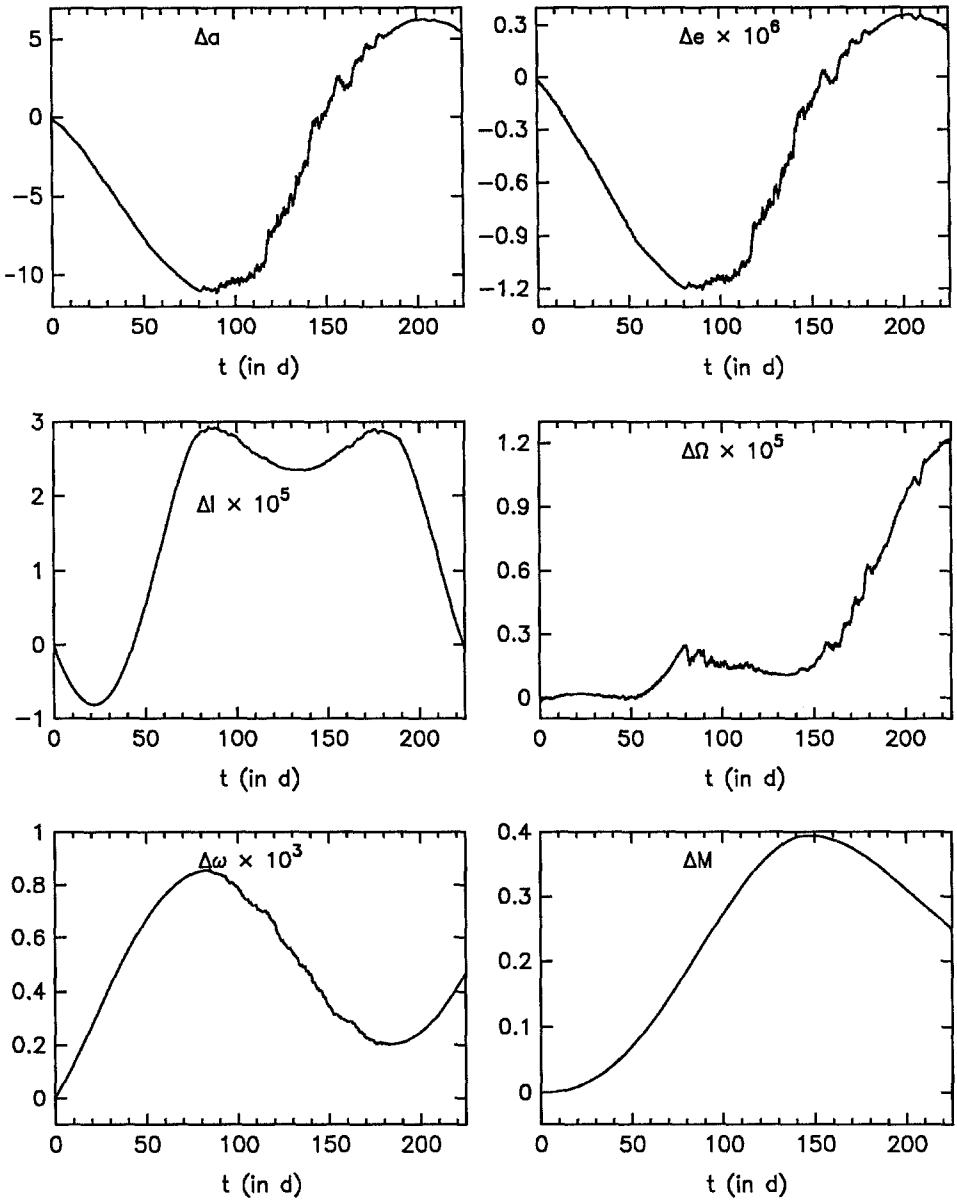

Fig. 14. Same as in figure 13, but over 225 days; Δa is now in m.

Acknowledgements

The research reported in this paper was accomplished while NB was a resident research associate at the Jet Propulsion Laboratory and PYL was a post-doctoral fellow at the California Institute of Technology. NB is very grateful to William Sjogren for stimulating this work, as well as for his interest and generous support. PYL acknowledges support by the NSF under grant AST 86–12799.

References

Anselmo, L., Farinella, P., Milani, A. and Nobili, A.M. : 1983, "Effects of the Earth-reflected Sunlight on the Orbit of the Lageos Satellite." *Astron. Astrophys.*, **117**, 3–8.

Baker, R.M.L. Jr. : 1966, "Radiation on a Satellite in the Presence of Partly Diffuse and Partly Specular Reflecting Body." In *Trajectories of Artificial Celestial Bodies* (J. Kovalevsky, Ed.), 85–150, Springer-Verlag, Berlin.

Barlier, F., Carpino, M., Farinella, P., Mignard, F., Milani, A. and Nobili, A.M. : 1986, "Non-gravitational perturbations on the semimajor axis of Lageos." *Ann. Geophys.*, **4A**, 193–210.

Knocke, P. and Ries, J. : 1987, "Earth Radiation Pressure Effects on Satellites." *Technical Memorandum CSR–TM–87–01*, Center for Space Research, the University of Texas at Austin, Austin, Texas.

Kabeláč, J. : 1988, "Radiation Influences of Higher Orders Acting on the Orbit of an Earth's Satellite." *Bull. Astron. Inst. Czechosl.*, **39**, 379–387.

Lautman, D.A. : 1977a, "Perturbations of a Close-Earth Satellite due to Sunlight Diffusely Reflected from the Earth. I : Uniform Albedo." *Celes. Mech.*, **15**, 387–420.

Lautman, D.A. : 1977b, "Perturbations of a Close-Earth Satellite due to Sunlight Diffusely Reflected from the Earth. II : Variable Albedo." *Celes. Mech.*, **16**, 3–25.

Levin, E. : 1962, "Reflected Radiation Received by an Earth Satellite.", *ARS Journal*, 1328–1331.

Lochry, R.R. : 1966, "The Perturbative Effects of Diffuse Radiations from the Earth and Moon on Close Satellites." *Ph. D. Thesis*, University of California at Los Angeles, 177 pp.

McCarthy, J.J. and Martin, T.V. : 1977, "A Computer Efficient Model of Earth Albedo Satellite Effects." *NASA Goddard Space Flight Center, Planetary Sciences Department Report no. 012–77.*

Milani, A., Nobili, A.M and Farinella, P. : 1987, *Non-Gravitational Perturbations and Satellite Geodesy*, Hilger, Bristol.

Morgan, W.J. : 1984, "Morning/Evening Difference in earth's albedo and the deceleration of Lageos." *EOS Trans. AGU*, **65**, p. 855.

Rubincam, D.P. : 1982, "On the Secular Decrease in the Semimajor Axis of Lageos's Orbit." *Celes. Mech.*, **26**, 361–382.

Rubincam, D.P. and Weiss, N.R. : 1986, "Earth Albedo and the Orbit of Lageos." *Celes. Mech.*, **38**, 233–296.

Rubincam, D.P. : 1987, "Lageos Orbit Decay Due to Infrared Radiation From Earth." *J. Geophys. Res.*, **92**, 1287–1294.

Rubincam, D.P., Knocke, P., Taylor, V.R. and Blackwell, S. : 1987, "Earth Anisotropic Reflection and the Orbit of Lageos." *J. Geophys. Res.*, **92**, 11662–11668.

Sehnal, L. : 1981, "Effects of the Terrestrial Infrared Radiation Pressure on the Motion of an Artificial Satellite." *Celes. Mech.*, **25**, 169–179.

Smith, D.E. : 1970, "Earth-Reflected Radiation Pressure." In *Dynamics of Satellites (1969)* (B. Morando, Ed.), 284–294, Springer-Verlag, Berlin.

Smith, D.E. and Dunn, P.J. : 1980, "Long Term Evolution of the Lageos Orbit." *Geophys. Res. Letters*, **7**, 437–440.

Smith, D.E. : 1983, "Acceleration on Lageos spacecraft." *Nature*, **304**, p. 15.

Taylor, F.W., Hunten, D.M., and Ksanfomaliti, L.V. : 1983, "The thermal balance of the middle and upper atmosphere of Venus." In *Venus* (D.M. Hunten, L. Colin, T.M. Donahue, and V.I. Moroz, Eds.), 650–680, University of Arizona Press, Tucson, Arizona.

Taylor, V.R., and Stowe, L.L. : 1984, "Reflectance Characteristics of Uniform Earth and Cloud Surfaces Derived from NIMBUS-7 ERB." *J. Geophys. Res.*, **89**, 4987–4996.